

[Chem. Pharm. Bull.]
31(9)2976—2985(1983)

Concurrent Adsorption of Calcium Ion and Hydroxyl Ion on Hydroxylapatite

SABURO SHIMABAYASHI* and MASAYUKI NAKAGAKI

*Faculty of Pharmaceutical Sciences, Kyoto University,
Yoshida-Shimoadachi-cho, Sakyo-ku,
Kyoto 606, Japan*

(Received February 7, 1983)

The amount of concurrent adsorption (*i.e.* co-adsorption) of Ca^{2+} and OH^- on hydroxyapatite (HAP) was determined. It was found that the amount of adsorption of OH^- (or Ca^{2+}) increases linearly with that of the other co-adsorbate, Ca^{2+} (or OH^-). Analysis of the data showed that there are two different adsorption sites on the surface of HAP: one is for individual ionic adsorption and the other is for ion-exchange and neutralization of proton. The adsorption isotherms for OH^- (or Ca^{2+}) were reduced to one curve when they were displaced somewhat in parallel with a straight line of slope -1 , taking the adsorbed amount of co-adsorbate, Ca^{2+} (or OH^-), into consideration. Adsorption of OH^- and Ca^{2+} and/or coordination of Ca^{2+} to the surface phosphate on HAP are considered to be similar to what occurs during the crystal growth of HAP.

Keywords—hydroxyapatite; calcium phosphate; hard tissue; biological mineralization; calcification; crystal growth; co-adsorption; adsorption of lattice ion; ion-exchange

Calcium phosphate in the form of hydroxyapatite (HAP , $\text{Ca}_{10}(\text{PO}_4)_6(\text{OH})_2$) is the main constituent of the skeletal system and of ectopic calcification. The biological HAP grows by capturing lattice ions from body fluid at the surface of HAP as a crystal nucleus and/or of amorphous calcium phosphate (ACP) as a precursor of HAP. Therefore, it seems important to study the adsorption of the lattice ions on HAP in an aqueous system. The majority of studies on the adsorption by HAP have dealt with the adsorption of only one species of adsorbate.

In the previous papers, it was shown that the amount of OH^- adsorption from an aqueous solution of $\text{Ca}(\text{OH})_2$ is higher than that from an aqueous solution of NaOH ,¹⁾ and that the amount of calcium adsorption increases with the amount of NaOH added (*i.e.* pH).²⁾ Furthermore, the equilibrium pH of an aqueous suspension of HAP decreases more upon the addition of CaCl_2 than of NaCl .^{1,3)} These results show that coexisting ions influence the amounts of adsorption of other ions on HAP, probably by co-adsorption.

In this work, the amounts of Ca^{2+} and OH^- adsorbed concurrently onto HAP from aqueous phase were determined. The results are discussed in terms of the interactions of these ions on adsorption.

Experimental

Material—HAP was prepared in the same manner as described elsewhere.⁴⁾ The product was a fine white powder. The X-ray powder diffraction pattern and infrared spectra were typical of HAP and chemical analysis showed that it was almost stoichiometric ($\text{Ca}/\text{P}=10/6$).

All chemicals used were of analytical grade, purchased from Nakarai Chemicals Ltd. or Wako Pure Chemical Industries Ltd. These were used without further purification. Water was doubly distilled.

Methods—The adsorbate solutions containing various concentrations of Ca^{2+} and OH^- were prepared by mixing aqueous solutions of CaCl_2 and KOH . However, care was always taken not to cause the precipitation of

$\text{Ca}(\text{OH})_2$ by taking its solubility product ($=5.5 \times 10^{-6} \text{ M}^3$) into consideration.⁵⁾ Care was also taken to avoid, as much as possible, contact of the sample solutions with atmospheric CO_2 by the use of N_2 gas in order to prevent the formation of CaCO_3 and consumption of OH^- .

HAP (2 g) was suspended in 20 ml of a given adsorbate solution of known concentration at 30°C , and shaken vigorously at frequent intervals. After at least 3 d, the Millipore filtrate (pore size $0.22 \mu\text{m}$) was used for chemical analysis.

Equilibrium concentration of OH^- was analyzed by the pH-titration method with a pH-meter (Toa type HM-5ES). It has been confirmed that phosphate ion dissolved from HAP does not interfere with the pH-titration because of the low solubility of HAP in the presence of excess amounts of Ca^{2+} and OH^- . Equilibrium concentration of Ca^{2+} was determined by EDTA chelatometry at pH 13 with 1-(2-hydroxy-4-sulfo-1-naphthylazo)-2-hydroxy-3-naphthoic acid (*i.e.* NN indicator). In the case of determining the free concentration of Ba^{2+} or Sr^{2+} , titration by EDTA chelatometry was done at pH 11 with 3,3'-bis-[*N,N*-di(carboxymethyl)-aminomethyl]-*o*-cresolphthalein (*i.e.* phthalein complexone) as an indicator. The equilibrium amount of adsorbed ion, x , expressed in units of moles per gram of HAP (mol/g-HAP), was basically calculated by the use of Eq. (1),

$$x = (c_i - c_f) \times 10^{-5} \quad (1)$$

where c_i and c_f are the adsorbate concentrations before and after adsorption (mM), and 10^{-5} is a numerical factor for conversion from the concentration difference to the amount of adsorption. Equation (1) can be modified to Eqs. (2), (3), (5), and (6), for particular species concerned. The adsorption of hydroxyl ion and metal ion studied in the present work was found to be reversible. Therefore, the amount of adsorption is independent of the order and speed of mixing of water, adsorbate solution, and HAP powder.

Results

Ion Adsorption and Counter Ion Effect

Adsorption isotherms for OH^- and/or M^{2+} ($=\text{Ca}^{2+}$, Sr^{2+} , or Ba^{2+}) from aqueous solutions of $\text{M}(\text{OH})_2$ and/or MCl_2 were determined. Total concentration of adsorbate M^{2+} plus Ca^{2+} , the latter having appeared from HAP by ion-exchange with the former,^{3,6)} was obtained as the apparent free concentration of M^{2+} by means of chelatometry with phthalein complexone as an indicator. However, the increase in Ca^{2+} concentration and the decrease in M^{2+} concentration due to ion-exchange cancel each other out. Therefore, the amount of adsorption of M^{2+} was calculated from the difference in the total concentration of metal ions analyzed before and after adsorption, where the effect of ion-exchange on the adsorption amount is neglected. It was confirmed that the amount of adsorption of $\text{M}(\text{OH})_2$ obtained by chelatometry (M^{2+} analysis) was in good agreement with that obtained by the pH-titration method (OH^- analysis).

Adsorption isotherms for OH^- are shown in Fig. 1(A), where the amount of adsorption

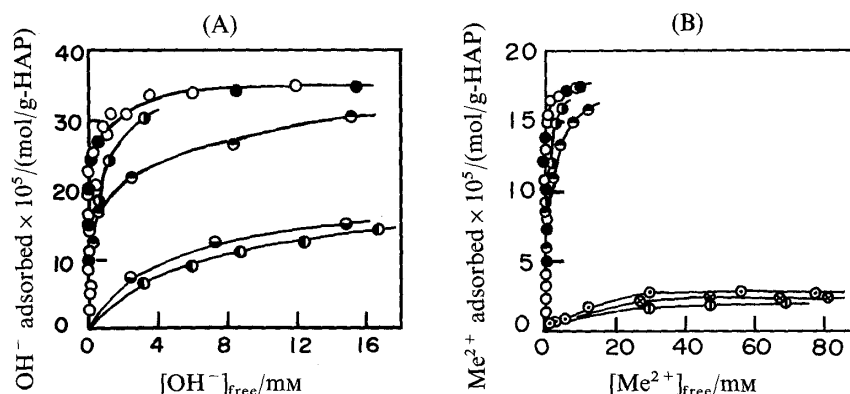


Fig. 1. (A): Adsorption Isotherms of Hydroxyl Ion from Various Hydroxides
(B): Adsorption Isotherms of Divalent Metal Ions from Various Chlorides and Hydroxides

○, $\text{Ca}(\text{OH})_2$; ●, $\text{Sr}(\text{OH})_2$; ⊙, $\text{Ba}(\text{OH})_2$; ○, CaCl_2 ; ⊗, SrCl_2 ; ⊕, BaCl_2 ; ●, NaOH ;
●, KOH .

Closed circles (●) are data from Figs. 2 and 3.

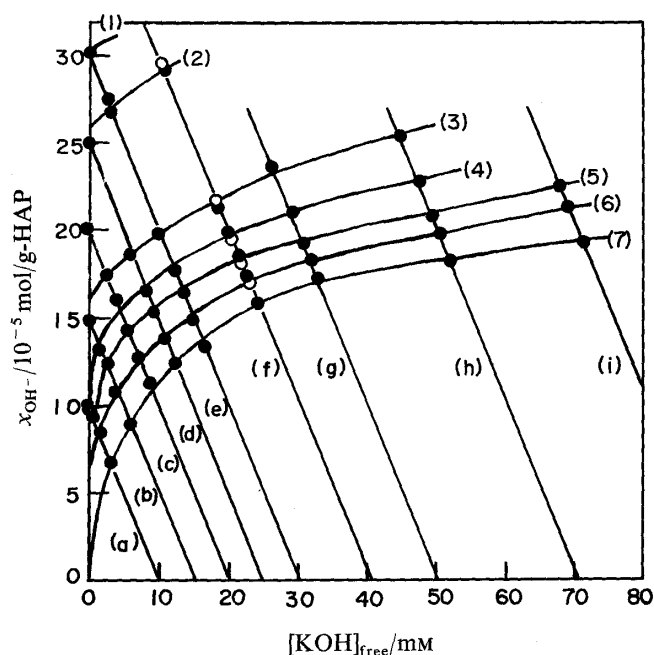


Fig. 2. Adsorption Isotherms of OH^- from Aqueous Solution of KOH Mixed with CaCl_2

Total concentration of CaCl_2 , $[\text{CaCl}_2]_t/\text{mM}$: (1), 32.7; (2), 13.5; (3), 6.5; (4), 3.4; (5), 2.5; (6), 1.0; (7), 0.

Total concentration of KOH, $[\text{KOH}]_t/\text{mM}$: (a), 10.0; (b), 15.0; (c), 20.1; (d), 25.0; (e), 30.2; (f), 40.2; (g), 50.3; (h), 70.4; (i), 90.5.

Equilibrium pH is 11–13.

Open and closed circles on the straight line (f) show the results of duplicate runs.

of OH^- from $\text{M}(\text{OH})_2$ is larger than that from NaOH or KOH .¹⁾ Adsorption isotherms for M^{2+} are also shown in Fig. 1(B), where the amount of adsorption from $\text{M}(\text{OH})_2$ is distinctly larger than that from MCl_2 . The order of amount of adsorption was obtained as follows: $\text{Ca}(\text{OH})_2 > \text{Sr}(\text{OH})_2 > \text{Ba}(\text{OH})_2$, and $\text{CaCl}_2 > \text{SrCl}_2 > \text{BaCl}_2$.

The above order coincides with that of the crystal ion radii of these cations: 0.99 Å (Ca^{2+}), 1.12 Å (Sr^{2+}), and 1.34 Å (Ba^{2+}). Ca^{2+} is most easily adsorbed on HAP because it is one of the lattice ions of HAP, and sites for M^{2+} -adsorption are mainly considered to be those formed by dislocations or defects of Ca^{2+} on HAP.³⁾ Sr^{2+} is more easily adsorbed on HAP than Ba^{2+} because the difference in crystal ion radii between Ca^{2+} and Sr^{2+} (=0.13 Å) is smaller than that between Ca^{2+} and Ba^{2+} (=0.35 Å).³⁾ The small difference found in the adsorbed amount of OH^- between NaOH and KOH in Fig. 1(A) can also be explained in the same manner (0.97 Å for Na^+ and 1.33 Å for K^+).³⁾ The reason why the adsorbed amount of M^{2+} from hydroxides is larger than that from chlorides is considered to be that OH^- is also one of the lattice ions of HAP, but Cl^- is not. It is known that the affinity of OH^- to HAP is higher than that of Cl^- .⁷⁾

Adsorption Isotherm of OH^- in the Presence of Ca^{2+}

The amount of OH^- adsorption, x_{OH^-} , on HAP is shown in Fig. 2 as a function of free concentration of KOH, $[\text{KOH}]_{\text{free}}$, at the adsorption equilibrium. In this case the equilibrium pH for almost all experimental points was pH 11–13. Curves (1)–(7) are adsorption isotherms where the total concentration of CaCl_2 , $[\text{CaCl}_2]_t$, added before adsorption is constant for each curve. Straight lines (a) through (i) show the relationship between x_{OH^-} and $[\text{KOH}]_{\text{free}}$ at constant concentration of total KOH added, $[\text{KOH}]_t$. According to Eq. (1), x_{OH^-} is expressed as follows:

$$x_{\text{OH}^-} = ([\text{KOH}]_t - [\text{KOH}]_{\text{free}}) \times 10^{-5} \quad (2)$$

Open and closed circles on the straight line (f) are experimental values for duplicate runs, which are in good agreement with each other and confirm the reproducibility of the data.

The amount of Ca^{2+} adsorbed concomitantly with OH^- was also determined from the same sample solution as that used for x_{OH^-} determination. The amount of Ca^{2+} adsorbed, $x_{\text{Ca}^{2+}}$, is calculated from Eq. (3) by taking account of the free concentration of CaCl_2 ,

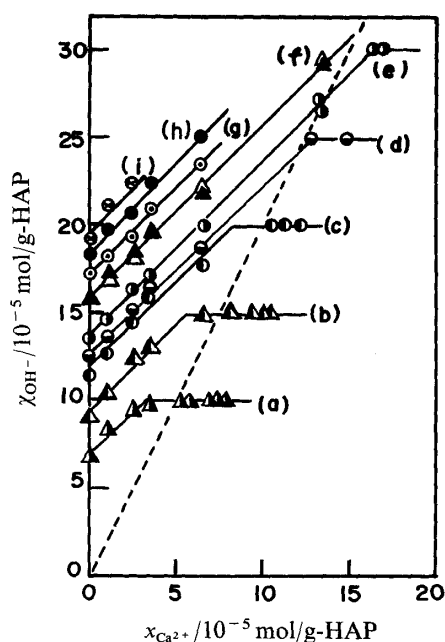


Fig. 3. Relationship between x_{OH^-} and $x_{\text{Ca}^{2+}}$ at Fixed $[\text{KOH}]_t$

The straight lines (a)–(i) in this figure correspond to the straight lines (a)–(i) in Fig. 2, respectively.

Open and closed triangles on the straight line (f) show the results of duplicate runs. The dotted line reflects the relation, $x_{\text{OH}^-} = 2x_{\text{Ca}^{2+}}$.

$[\text{CaCl}_2]_{\text{free}}$,

$$\begin{aligned} x_{\text{Ca}^{2+}} &= ([\text{CaCl}_2]_t - [\text{CaCl}_2]_{\text{free}}) \times 10^{-5} \\ &= [\text{CaCl}_2]_b \times 10^{-5} \end{aligned} \quad (3)$$

where $[\text{CaCl}_2]_b$ is the amount of CaCl_2 adsorbed expressed in concentration unit. The relationship between x_{OH^-} and $x_{\text{Ca}^{2+}}$ at fixed $[\text{KOH}]_t$ is shown in Fig. 3, where x_{OH^-} increases linearly with $x_{\text{Ca}^{2+}}$ and levels off with a sharp break when almost all of the added OH^- in the solution is consumed by adsorption. In other words, $x_{\text{Ca}^{2+}}$ increases initially with x_{OH^-} , and finally without further increase of x_{OH^-} after the break point. The break point in Fig. 3 corresponds to the intersecting point of the straight line with the ordinate in Fig. 2 (*i.e.* x_{OH^-} at $[\text{KOH}]_{\text{free}} = 0$). Almost all of the Ca^{2+} added is adsorbed on HAP when $[\text{KOH}]_t$ is large compared with $[\text{CaCl}_2]_t$. The region where all of the added Ca^{2+} is exhausted is located over a wide range between the ordinate and the break point for each straight line in Fig. 3, or is located on each straight line (a)–(i), except for $[\text{KOH}]_{\text{free}} = 0$, in Fig. 2.

Slopes of all the straight lines drawn between the break point and the ordinate in Fig. 3 are approximately 1. Therefore, the straight line can be expressed by Eq. (4),

$$x_{\text{OH}^-} = x_{\text{OH}^-}^0 + m x_{\text{Ca}^{2+}} \quad (4)$$

where m ($=1$) is the slope and $x_{\text{OH}^-}^0$, the intercept of the ordinate, is the amount of OH^- adsorbed when $x_{\text{Ca}^{2+}} = 0$ and/or $[\text{CaCl}_2]_t = 0$. This value of $x_{\text{OH}^-}^0$ indicates the inherent amount of adsorption of OH^- on HAP without the aid of adsorbed Ca^{2+} (*i.e.* curve (7) in Fig. 2).

The dotted line in Fig. 3 shows the relationship $x_{\text{Ca}^{2+}}/x_{\text{OH}^-} = 1/2$. When $\text{Ca}(\text{OH})_2$ is adsorbed from its aqueous solution with or without an indifferent electrolyte, the experimental points should be on this dotted line. Closed circles (●) shown in Fig. 1(A) are the amount of adsorption of OH^- taken from the intersecting points of the dotted line with the straight lines in Fig. 3. The free concentration of OH^- , to which the adsorption amount corresponds, can be obtained from the adsorption isotherm shown in Fig. 2. These data (●) are concordant with the data shown by the open circles (○) in Fig. 1(A), which were determined by direct analysis of $\text{Ca}(\text{OH})_2$ itself. It may, therefore, be concluded that the amount of OH^- adsorption from the aqueous solution of KOH mixed with CaCl_2 under the condition

$x_{\text{Ca}^{2+}}/x_{\text{OH}^-} = 1/2$ is almost the same as that measured in the aqueous solution of $\text{Ca}(\text{OH})_2$, and that coexisting ions, such as K^+ and Cl^- originated from KOH and CaCl_2 , have very little effect on the amount of adsorption of OH^- .

In the region on the right-hand side of the dotted line in Fig. 3, the net electric charge on the surface of HAP is expected to be positive owing to the fact that $2x_{\text{Ca}^{2+}} > x_{\text{OH}^-}$. This was confirmed by means of electrophoresis, as mentioned in the previous papers.^{1,2)} Mishra *et al.*⁸⁾ also found that HAP particles have positive surface charge in an aqueous phase (pH 7–10) containing excess Ca^{2+} , although HAP should have negative surface charge on the basis of the point of zero charge obtained in aqueous phase without Ca^{2+} .

Adsorption Isotherms of Ca^{2+} in the Presence of OH^-

The amount of Ca^{2+} adsorbed, $y_{\text{Ca}^{2+}}$, on HAP is shown in Fig. 4 as a function of free concentration of CaCl_2 , $[\text{CaCl}_2]_{\text{free}}$, in the presence of KOH , the concentration of which is $[\text{KOH}]_i$. In this case the equilibrium pH of the solution was pH 6–7, which is lower than that in the case of Fig. 2. Some portion of the total Ca^{2+} added remains in solution at pH 6–7 as free CaCl_2 when the adsorption equilibrium is attained, though almost all of the Ca^{2+} added was adsorbed on HAP from the solution at high pH (pH 11–13), as mentioned before (Fig. 2 or 3). In this section the amounts of adsorption of Ca^{2+} and OH^- will be represented by y to distinguish them from those at higher pH (11–13) described previously.

Curves (1) through (6) were obtained at constant $[\text{KOH}]_i$. Straight lines (a) through (i) show the relationship between $y_{\text{Ca}^{2+}}$ and $[\text{CaCl}_2]_{\text{free}}$ at a fixed concentration of added CaCl_2 , $[\text{CaCl}_2]_i$. These straight lines are expressed, according to Eq. (1), as follows:

$$y_{\text{Ca}^{2+}} = ([\text{CaCl}_2]_i - [\text{CaCl}_2]_{\text{free}}) \times 10^{-5} \quad (5)$$

The adsorption isotherms (1) through (6) seem to be parallel with each other. The results in Figs. 4 and 2 will be discussed later.

The amount of OH^- adsorbed simultaneously with Ca^{2+} was also determined with the same sample solution as that used for $y_{\text{Ca}^{2+}}$, according to Eq. (6),

$$\begin{aligned} y_{\text{OH}^-} &= ([\text{KOH}]_i - [\text{KOH}]_{\text{free}}) \times 10^{-5} \\ &= [\text{KOH}]_b \times 10^{-5} \end{aligned} \quad (6)$$

where $[\text{KOH}]_b$ is the decrease in the concentration of added KOH due to adsorption. The relationship between $y_{\text{Ca}^{2+}}$ and y_{OH^-} at fixed $[\text{CaCl}_2]_i$ is shown in Fig. 5, where $y_{\text{Ca}^{2+}}$ in-

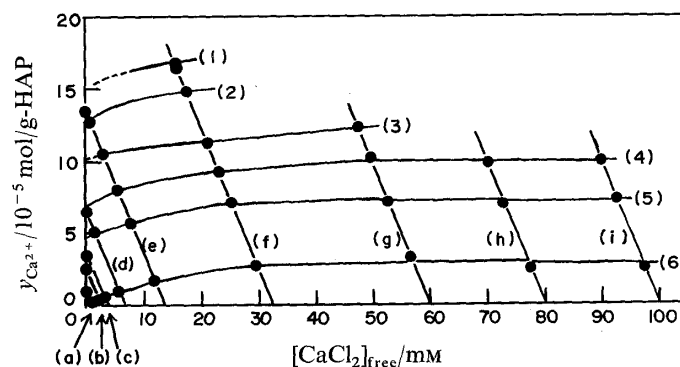


Fig. 4. Adsorption Isotherms of Ca^{2+} from Aqueous Solution of CaCl_2 Mixed with KOH

Total concentration of KOH , $[\text{KOH}]_i/\text{mM}$: (1), 30.2; (2), 25.0; (3), 20.1; (4), 15.0; (5), 10.0; (6), 0.

Total concentration of CaCl_2 , $[\text{CaCl}_2]_i/\text{mM}$: (a), 1.0; (b), 2.5; (c), 3.4; (d), 6.5; (e), 13.5; (f), 32.7; (g), 60.0; (h), 80.0; (i), 100.

Equilibrium pH is 6–7.

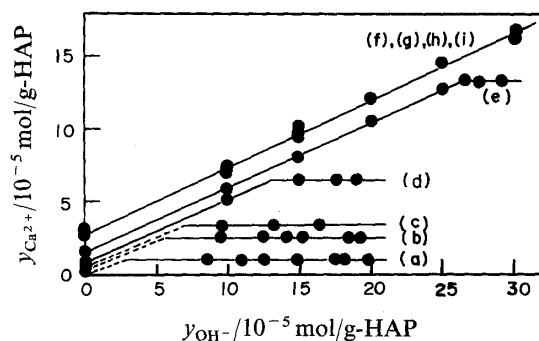


Fig. 5. Relationship between y_{OH^-} and $y_{Ca^{2+}}$ at Fixed $[CaCl_2]_t$

The straight lines (a)—(i) correspond to the straight lines (a)—(i) in Fig. 4, respectively.

creases linearly with increase of y_{OH^-} then levels off with a sharp break when all of the added Ca^{2+} is exhausted by adsorption. In other words, y_{OH^-} continues to increase even when $y_{Ca^{2+}}$ has ceased to increase. The break points in Fig. 5 are related to the intersecting points of the straight lines with the ordinate in Fig. 4, where $[CaCl_2]_{free} = 0$.

Almost all of the OH^- added is adsorbed on HAP when $[KOH]_t$ is comparatively small compared with $[CaCl_2]_t$. Therefore, the equilibrium pH of the solution became almost neutral (pH 6—7) even though considerable KOH, $[KOH]_t$, had been added to the solution before the adsorption. The region where complete consumption of OH^- added occurs is located between the ordinate and the break point of the straight line for each $[CaCl_2]_t$ in Fig. 5. On the other hand, the region where free OH^- still remains in the solution at the adsorption equilibrium is located on the horizontal portion of each line (a)—(i) in Fig. 5. This horizontal portion, where Ca^{2+} in the solution is completely consumed by adsorption and the amount of OH^- adsorption is still increasing, corresponds to the region where the adsorption isotherm for OH^- , as shown in Fig. 2, is obtained. In the same manner, horizontal branches in Fig. 3 correspond to the region where the adsorption isotherm for Ca^{2+} , as shown in Fig. 4, is obtained.

All straight lines in Fig. 5 (excluding the horizontal portion) may be expressed by Eq. (7),

$$y_{Ca^{2+}} = y_{Ca^{2+}}^0 + n y_{OH^-} \quad (7)$$

where n is the slope ($=0.45-0.47$) and $y_{Ca^{2+}}^0$, the intercept of the ordinate, is the value of $y_{Ca^{2+}}$ at $y_{OH^-} = 0$ and $[KOH]_t = 0$, namely, the amount of Ca^{2+} adsorption on curve (6) in Fig. 4. This value, $y_{Ca^{2+}}^0$, shows the amount of Ca^{2+} adsorbed on HAP without cooperation of OH^- adsorption.

Reduction of the Adsorption Isotherms to One Curve

From Eqs. (2)—(4), and Eq. (2) modified by replacing x_{OH^-} and $[KOH]_{free}$ with $x_{OH^-}^0$ and $[KOH]_{free}^0$, the following equations can be obtained, where $[KOH]_{free}^0$ is the equilibrium concentration of KOH when $CaCl_2$ is not added:

$$x_{OH^-}^0 = x_{OH^-} - m x_{Ca^{2+}} \quad (4')$$

and

$$[KOH]_{free}^0 = [KOH]_{free} + m [CaCl_2]_b \quad (8)$$

In the same manner, the following equations are obtained from Eqs. (5)—(7):

$$y_{Ca^{2+}}^0 = y_{Ca^{2+}} - n y_{OH^-} \quad (7')$$

and

$$[CaCl_2]_{free}^0 = [CaCl_2]_{free} + n [KOH]_b \quad (9)$$

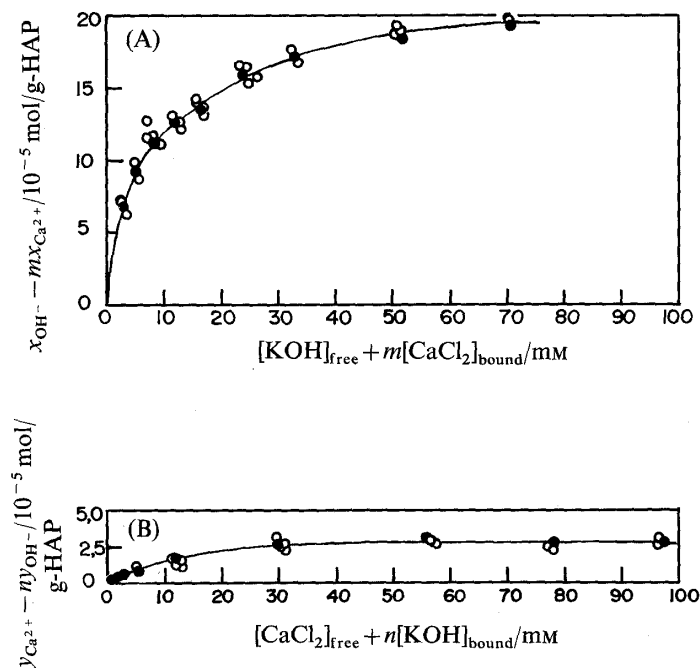


Fig. 6. (A): Reduced Adsorption Isotherm for OH^-
(B): Reduced Adsorption Isotherm for Ca^{2+}

where $[CaCl_2]_{free}^0$ is the equilibrium concentration of $CaCl_2$ in the absence of KOH .

Equations (4)' and (8) mean that the relationship between x_{OH^-} and $[KOH]_{free}$ in Fig. 2 should coincide with that between $x_{OH^-}^0$ and $[KOH]_{free}^0$ (where $[CaCl_2]_t = 0$) if the curves are transferred by $m x_{Ca^{2+}}$ downwards and by $m[CaCl_2]_b$ to the right-hand side. Figure 6(A) shows the relationship between $x_{OH^-} - m x_{Ca^{2+}}$ and $[KOH]_{free} + m[CaCl_2]_b$, according to Eqs. (4)' and (8). The closed circles and the solid line are experimental data taken from curve (7) in Fig. 2 (i.e. $x_{OH^-}^0$ vs. $[KOH]_{free}^0$) and open circles are recalculated points from curves (1) through (6) in Fig. 2. These data fall almost on one curve, as expected from Eqs. (4)' and (8). However, the data on the ordinate in Fig. 2, that is, on the horizontal portion in Fig. 3 deviate from the reduced curve, because Eqs. (4) or (4)' is not applicable to them. These data are omitted in Fig. 6(A).

In the same manner, the adsorption isotherms shown in Fig. 4 are reduced to one adsorption isotherm by means of Eqs. (7)' and (9), as shown in Fig. 6(B). Some of the data from Fig. 4 deviate from the reduced adsorption isotherm for the same reason as mentioned above, that is, inapplicability of Eqs. (7) or (7)'. These data are not shown in Fig. 6(B).

Therefore, the adsorption isotherms shown in Figs. 2 and 4 may be regarded as somewhat displaced in parallel by the effect of co-adsorption of Ca^{2+} and OH^- , and not as an example of the high affinity type having a steep initial slope.

Discussion

Co-adsorption of Ions

The amount of OH^- or Ca^{2+} adsorbed from $Ca(OH)_2$ is larger than that from $NaOH$ or KOH (Fig. 1(A)) or from $CaCl_2$ (Fig. 1(B)). In these cases, almost all of the Na^+ , K^+ , or Cl^- may be distributed in the diffuse electric double layer in order to maintain electroneutrality but may not significantly come into contact with the surface of HAP, because the affinity of Na^+ , K^+ , or Cl^- to HAP is distinctly smaller than that of Ca^{2+} or OH^- , as mentioned before.^{1,3,7)} As for the system of $Ca(OH)_2$, both Ca^{2+} and OH^- are easily adsorbed on HAP,

because both of them are the lattice ions of HAP. It is reasonable to consider that the adsorption of Ca^{2+} forms adsorption sites for hydroxyl ion, and *vice versa*. Therefore, coexistence of these ions increases the adsorption of both, through supplying additional adsorption sites and through electrostatic attractive force. Consequently, the amounts of adsorption of Ca^{2+} and OH^- from $\text{Ca}(\text{OH})_2$ are larger than those from other systems such as CaCl_2 or NaOH , as shown in Fig. 1.

Co-adsorption phenomena have been noticed by several authors: that of Ca^{2+} with phosphate ion or hydroxyl ion to HAP was found by means of electrokinetic measurement (zeta potential measurement) by Fuerstenau *et al.*^{8,9)} and that of tetraalkylammonium ion (TAA^+) and nitrate ion to the silver iodide surface was pointed out by De Keizer *et al.*,¹⁰⁾ who concluded that nonnegligible co-adsorption of NO_3^- , located in the Stern layer between TAA^+ ions, contributes to the lateral screening. These authors, however, did not measure the amount of adsorption of each co-adsorbate. We have now done this in the case of co-adsorption by HAP.

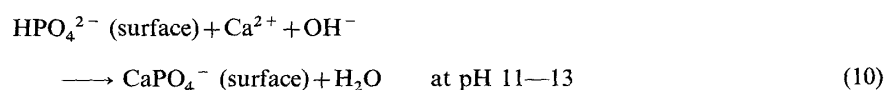
Mechanism of Co-adsorption of Ca^{2+} and OH^- by HAP

Davis *et al.*¹¹⁾ showed that metal ions (M^{2+}), which are adsorbed on the surface of metal oxide, easily bind OH^- and form MOH^+ (Pb^{2+} and PbOH^+ on the surface of $\gamma\text{-Al}_2\text{O}_3$, for example). This may be assumed to be co-adsorption of M^{2+} and OH^- . The formation of MOH^+ , however, is explained by the fact that metal ions are more easily hydrolyzed at the surface than in the bulk water. Van Riemsdijk *et al.*¹²⁾ studied the interaction of phosphate ion with gibbsite ($\text{Al}(\text{OH})_3$), and observed the formation of taranakite ($\text{H}_6\text{K}_3\text{Al}_5(\text{PO}_4)_8 \cdot 18\text{H}_2\text{O}$) on the surface of gibbsite under certain conditions. Phosphate uptake by gibbsite, therefore, occurs due to ordinary adsorption and precipitation.

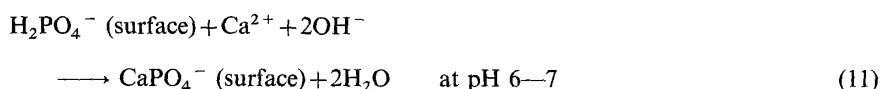
In the present work, the possibility of the formation of hydrolyzed species (CaOH^+) as well as precipitation ($\text{Ca}(\text{OH})_2$) can be excluded because of the experimental conditions used. Accordingly, co-adsorption in the present work is caused neither by hydrolysis of Ca^{2+} nor by precipitation of $\text{Ca}(\text{OH})_2$.

In the previous paper,¹³⁾ it was found that the amount of OH^- adsorption on HAP treated with $(\text{NH}_4)_2\text{HPO}_4$ is larger than that on untreated HAP. The increase of OH^- adsorption caused by pre-adsorbed phosphate ion seems strange in view of the electrostatic repulsion between OH^- anion as the adsorbate and phosphate anion on the surface. However, it can be explained by considering that, instead of direct adsorption of OH^- , consumption of OH^- occurs by protons dissociated from protonated phosphate ions which have been pre-adsorbed on the surface of HAP. A similar explanation may be applied to the co-adsorption found in the present work.

According to Eqs. (4) and (7), an increase in the amount of Ca^{2+} adsorption by 1 mol accompanies an increase of the amount of OH^- adsorption by 1 mol ($=m$ at pH 11–13) or by 2.1–2.2 mol ($=1/n$ at pH 6–7) due to co-adsorption. Taking into account the fact that the pK values for the dissociation constants of phosphate in the bulk water, pK_1 , pK_2 , and pK_3 are 2.12, 7.21, and 12.52, respectively,¹⁴⁾ and that the extent of dissociation of phosphate ion on the surface may be smaller than that in the bulk water, the dominant ionic species of phosphate exposed on the surface may be assumed to be HPO_4^{2-} (pH 11–13) or H_2PO_4^- (pH 6–7). When Ca^{2+} and OH^- as adsorbate ions come in contact with the surface of HAP, the following ion-exchange and neutralization reactions are assumed to occur:

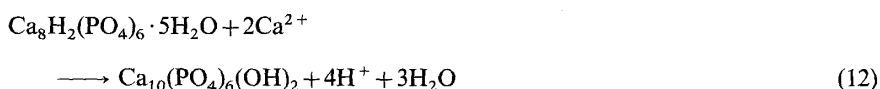


and



It is not clear whether the ion-exchange causes the neutralization reaction or whether the dissociation and neutralization of a proton cause the binding of calcium ion to the surface phosphate. In either case, according to reactions (10) and (11), ion-exchange of H^+ with Ca^{2+} is accompanied with consumption of 1 mol or 2 mol of OH^- through the neutralization reaction. These values (1 or 2) are approximately equal to the experimental values ($m=1$ in Eq. (4), or $1/n=2.1\text{—}2.2$ in Eq. (7)).

Brown *et al.*¹⁵⁾ studied the reaction of calcium ion with octacalcium phosphate (OCP), which is regarded as a precursor in the formation of the hard-tissue mineral, HAP. This OCP is unstable relative to HAP and tends to hydrolyze to HAP according to reaction (12):



where 4 mol of H^+ is liberated from OCP with consumption of 2 mol of Ca^{2+} . In the case where H^+ is neutralized by OH^- , the ratio of consumption of Ca^{2+} to OH^- becomes 1/2, as in reaction (11). However, the sample HAP used in the present work was prepared carefully to avoid by-products formation during the reaction period of many days, and was "ripened" thoroughly.⁴⁾ Therefore, both possibilities (presence of OCP as a contaminant in the sample HAP, and surface coating by OCP on HAP) are very unlikely. However, consumption of H^+ from OCP and subsequent substitution of Ca^{2+} in the bulk reaction (12) is similar to the surface reactions (10) and (11).

In conclusion, two mechanisms of co-adsorption may operate simultaneously in the present case: the one is concurrent real adsorption of Ca^{2+} and OH^- at appropriate adsorption sites, and the other is concomitant reactions of ion-exchange and neutralization. Binding sites for Ca^{2+} are protonated surface phosphates characterized by the reactions (10) and (11), and Ca^{2+} -defects in the neighborhood of phosphate or hydroxyl ion on the HAP surface.³⁾ Ca^{2+} binds or co-ordinates to these lattice anions of HAP. Adsorption sites for OH^- are OH^- -defects in the neighborhood of Ca^{2+} on the HAP surface.¹⁾ Consumption of OH^- by the reaction (10) and (11) should also be considered. Thus, the co-adsorption, as well as individual ion adsorptions of Ca^{2+} and OH^- , on the HAP surface is similar to what occurs during the crystal growth of HAP. Replacement of surface protons by Ca^{2+} , as shown in reactions (10) and (11), appears to be convenient for the crystal growth of HAP. Hard-tissue formation or biological mineralization of HAP may occur in a similar manner with phosphate ion in addition to Ca^{2+} and OH^- .

Acknowledgement We are grateful to Mr. K. Kimura, Faculty of Technology, Kyoto University, for measuring the X-ray powder diffraction patterns of HAP.

References

- 1) S. Shimabayashi, C. Tamura, and M. Nakagaki, *Chem. Pharm. Bull.*, **29**, 3090 (1981).
- 2) S. Shimabayashi, C. Tamura, and M. Nakagaki, *Yakugaku Zasshi*, **102**, 137 (1982).
- 3) S. Shimabayashi, C. Tamura, and M. Nakagaki, *Chem. Pharm. Bull.*, **29**, 2116 (1981).
- 4) S. Shimabayashi and M. Nakagaki, *Nippon Kagaku Kaishi*, **1978**, 326; Y. Avnimelech, E. C. Moreno, and W. E. Brown, *J. Res. Nat. Bur. Stand.*, **77**, 149 (1973).
- 5) The Chemical Society of Japan (ed.), "Kagaku Binran, Kiso-Hen," 2nd ed., Maruzen, Tokyo, 1975, p. 800.
- 6) T. Suzuki, T. Hatsushika, and Y. Hayakawa, *J. Chem. Soc., Faraday Trans. 1*, **77**, 1059 (1981); T. Suzuki, T. Hatsushika, and M. Miyake, *J. Chem. Soc., Faraday Trans. 1*, **78**, 3605 (1982).
- 7) S. Shimabayashi, T. Kondo, and M. Nakagaki, *Yakugaku Zasshi*, **103**, 391 (1983).
- 8) R. K. Mishra, S. Chander, and D. W. Fuerstenau, *Colloid and Surfaces*, **1**, 105 (1980).

-
- 9) S. Chander and D. W. Fuerstenau, *Colloids and Surfaces*, **4**, 101 (1982).
 - 10) A. De Keizer and J. Lyklema, *J. Colloid Interface Sci.*, **75**, 171 (1980).
 - 11) J. A. Davis and J. O. Leckie, *J. Colloid Interface Sci.*, **67**, 90 (1978).
 - 12) W. H. Van Riemsdijk and J. Lyklema, *J. Colloid Interface Sci.*, **76**, 55 (1980).
 - 13) S. Shimabayashi, H. Fukuda, T. Aoyama, and M. Nakagaki, *Chem. Pharm. Bull.*, **30**, 3074 (1982).
 - 14) P. G. Stecher (ed.), "The Merck Index," 8th ed., Merck and Co., Inc., Rahway, N.J., 1968, p. 824.
 - 15) W. E. Brown, L. W. Schroeder, and J. S. Ferris, *J. Phys. Chem.*, **83**, 1385 (1979).